

The effect of a strong external field on the electronic dephasing of a solute that is strongly coupled to a solvent

Cite as: J. Chem. Phys. **111**, 5408 (1999); <https://doi.org/10.1063/1.479801>

Submitted: 19 March 1999 . Accepted: 28 June 1999 . Published Online: 10 September 1999

R. I. Cukier, C. Denk, and M. Morillo



View Online



Export Citation

Lock-in Amplifiers
up to 600 MHz



The effect of a strong external field on the electronic dephasing of a solute that is strongly coupled to a solvent

R. I. Cukier^{a)}

Department of Chemistry and Center for Fundamental Materials Research, Michigan State University, East Lansing, Michigan 48824-1322

C. Denk

Física Teórica, Universidad de Sevilla, Apartado de Correos 1065, Sevilla 41080, Spain

M. Morillo

Department of Chemistry and Center for Fundamental Materials Research, Michigan State University, East Lansing, Michigan 48824-1322 and Física Teórica, Universidad de Sevilla, Apartado de Correos 1065, Sevilla 41080, Spain

(Received 19 March 1999; accepted 28 June 1999)

A recent theory of strong field spectroscopy (SFS) [R. I. Cukier and M. Morillo, *Phys. Rev. B* **57**, 6972 (1998), M. Morillo and R. I. Cukier, *J. Chem. Phys.* (**110**, 7966 (1999))] is generalized to apply to strong solute–solvent coupling. In SFS, a strong external field is used to connect, with the transition dipole, two electronic states of a solute immersed in a medium. In contrast to weak fields, $\bar{z}(t)$, the average population difference of the solute electronic states is changing significantly. For resonant, strong fields, $\bar{z}(t)$ and the average absorbed power, $\bar{P}(t)$, exhibit oscillatory decays in time that reflect the changing $\bar{z}(t)$ and the dissipation arising from the coupling to the medium. When the solute–solvent coupling is relatively weak, the time evolution of the solvent only depends on the initial solute state (autonomous behavior). In this work, appropriate to strong coupling, we derive an equation of motion for the solvent dynamics that depends on the solute's instantaneous state (nonautonomous behavior). The consequences to $\bar{z}(t)$ and $\bar{P}(t)$ are explored. We find that instead of equalizing the solute populations at long times, now the population is inverted relative to its initial state. We also find that the degree of long-time population inversion can be controlled by turning off the external field before the system has fully relaxed. © 1999 American Institute of Physics.

[S0021-9606(99)50936-7]

I. INTRODUCTION

The interrogation by optical spectroscopy of a solute in a solvent provides information on their interactions.^{1–6} Such studies have been carried out in liquids,^{7–9} crystals,^{3,10} glasses,^{3,6,11} and proteins.^{12,13} The broadening of the optical transition that is typically observed mirrors the differing local environments that the solute experiences in the presence of the solvent. When the solute's electronic distribution is quite different in the optically connected states, and when the coupling of the solute charge distribution to the solvent is strong, dramatic effects on the optical spectrum are anticipated.²

Another aspect of the interaction of external fields with atoms and molecules that is under intense study is the desire to control the fate of some process in the moiety coupled to the field. This may involve controlling the outcome of the final state population in a chemical transformation,^{14–17} or tunneling populations in two-level^{18–20} and multi-level systems.^{21,22} For example, we have shown how the application of suitable external electric fields can be used to create

and maintain desired populations of localized states in hydrogen-bonded proton tautomers.¹⁹

The original studies of optical spectra were carried out with weak external fields so that linear response theory (LRT)²³ could be applied.^{24–26} Then, only the material properties are relevant, i.e., the linear susceptibility is independent of the external field. Subsequently, various nonlinear optical (NLO) spectroscopic methods were developed to obtain more detailed information about the material properties.^{1–13} For example, because linear spectroscopy cannot discriminate between homogeneous and inhomogeneous broadening mechanisms, hole-burning^{1,27} and echo^{4,28} experiments were developed to access the homogeneous contribution to the linewidth. The NLO techniques are perturbative in the external field strength and, with regard to the analysis of such experiments, involve higher order susceptibilities. Relating these susceptibilities to a microscopic model of the material then introduces multi-point time correlation functions, and leads to nontrivial analyses to connect theory and experiment.²

In a recent series of articles^{29,30} we have introduced a new, nonperturbative approach to optical spectroscopy, referred to as strong field spectroscopy (SFS), that does not rely on perturbation theory in the external field. A Hamil-

^{a)}Electronic mail: cukier@argus.cem.msu.edu

tonian for a two-state system coupled to a solvent, modeled as an oscillator bath, was analyzed.³⁰ The coupling of the external field to the transition dipole of the solute is sufficiently strong that a perturbative analysis is precluded. We obtained approximate equations of motion for this system that were analyzed by a combination of analytic and numerical methods. The solvent was assumed to be classical and that permitted its representation as a stochastic process. In such solute–solvent coupled problems there are several key parameters: the reorganization energy E_r , the solvent relaxation time τ_c , and the temperature T . E_r measures the energetic displacement of the solvent and τ_c is the solvent's characteristic relaxation time that gauge the response to the solute's differing electronic structure in its initial and final states. The parameter $\Delta = \sqrt{2E_r k_B T / \hbar^2}$ is a bandwidth that measures the ability of the thermal fluctuations to provide differing solute–solvent interaction energies. When the coupling to the external field is strong, the populations of the two states are changing significantly. It is this changing population that distinguishes SFS from LRT and NLO spectroscopy where, implicitly or explicitly, the assumption is made of infinitesimal perturbation of the solute's initial state population. When the population is changing, we found that the equations of motion previously obtained are valid for $\hbar\Delta < E_r$. This restriction leads to autonomous equations of motion, whereby the solvent's dynamics only depends on the solute's initial state. There is no feedback from the solute's changing state to the solvent's dynamics. With this autonomous dynamics for the solvent, the analysis of its influence on the solute dynamics is greatly simplified. For fast modulation, $\Delta\tau_c < 1$,^{31,32} we were able to obtain essentially analytic results,²⁹ while for slow modulation, $\Delta\tau_c > 1$, a numerical analysis was required.³⁰ The (time dependent) average power absorbed by the sample $\bar{P}(t)$ was evaluated. The spectrum of this quantity consists of three peaks: one at low frequency and two centered on twice the applied frequency, ω_0 , and symmetrically displaced from $2\omega_0$ in proportion to the strength of the external field transition dipole coupling. The widths of the peaks reflect the “dissipation” (dephasing) from coupling to the solvent.

The condition $E_r < \hbar\Delta$ restricts the applicability of SFS to nonpolar or weakly polar solvents, where the reorganization energy is small compared with the thermal fluctuations, i.e., $E_r/\hbar\Delta \propto \sqrt{E_r/k_B T} < 1$.¹⁰ In polar solvents, the opposite inequality is more likely to be obeyed.³³ Thus, it is important to extend our SFS to be applicable to this regime, and we do so in this article. A new set of equations of motion are developed that can account for the dynamic feedback of the solute's changing population on the solvent's evolution. The solvent's evolution is then nonautonomous, and this greatly complicates the analysis. The consequences to the total system's evolution of this nonautonomous dynamics are profound. Before, for autonomous dynamics, we found that $\bar{z}(t)$ showed an oscillatory decay to zero; ultimately the populations of the two states are equalized because of the decoherence brought about by the solute's interaction with the solvent. Now, $\bar{z}(t)$ goes to a nonzero limit, thus providing unequal populations of the electronic states. The power ab-

sorbed is also modified in a way that will be detailed below. The feature that the long-time population is not equalized suggests the interesting possibility of controlling the population with the use of SFS. We shall see that this is indeed possible, even though the solute is coupled to the solvent. Clearly, controlling such populations in the presence of thermal fluctuations is not as straightforward as for an isolated solute.

The plan of the rest of this paper is as follows: In Sec. II, we review the Hamiltonian appropriate to describe electronic dephasing of a two-level system, representing the solute, coupled to a solvent and to a strong external field. The new equations of motion that are applicable to the $E_r > \hbar\Delta$ regime are obtained. In Sec. III, the equations of motion are analyzed by a numerical scheme appropriate to the solution of nonautonomous stochastic differential equations. We discuss the implications of the solutions of the equations of motion. In Sec. IV, we analyze a set of deterministic equations that follow from the stochastic set, to show that the main features of the nonautonomous evolution is present even when the fluctuations are ignored. In Sec. V, we show how properly constructed external fields can control the solute's long-time population. Our concluding remarks are presented in Sec. VI.

II. THE HAMILTONIAN AND APPROXIMATE EQUATIONS OF MOTION

A model Hamiltonian that can be used to characterize electronic dephasing is:^{24,34–36}

$$\mathcal{H} = \sum_j \frac{p_j^2}{2m_j} + \frac{1}{2} m_j \omega_j^2 \left(q_j - \frac{\gamma_j}{m_j \omega_j^2} \sigma_z \right)^2 - \frac{\Delta G^0}{2} \sigma_z + 2\hbar b(t) \sigma_x. \quad (1)$$

The solute has two electronic states here denoted by the kets $|0\rangle$ and $|1\rangle$. The solvent is represented by a set of independent harmonic oscillators whose origins depend substantially upon the electronic state of the solute. These shifts reflect the differing interaction energies between the two charge distributions of the solute with the solvent. The σ_i ($i=x,y,z$) are the Pauli spin operators. Once the solute is reduced to only two active states it can be described by a spin variable, and we shall use solute and spin language interchangeably. The external field–solute interaction energy is defined by $2\hbar b(t) = \langle 0|\hat{\mu}|1\rangle \cdot \mathbf{E}(t)$, where $\hat{\mu}$ is the solute's dipole moment operator and $\mathbf{E}(t)$ is the external field. The quantity ΔG^0 is the standard free energy difference between reactants and products. The m_j 's and ω_j 's are, respectively, the oscillator masses and frequencies, and the γ_j 's are the solute–solvent coupling constants. Using the Heisenberg equation of motion for the operator \mathcal{O} ,

$$i\hbar \dot{\mathcal{O}} = [\mathcal{O}, \mathcal{H}], \quad (2)$$

we obtain for the Pauli operators the equations

$$\dot{\sigma}_x(t) = \frac{2}{\hbar} \sum_j \gamma_j q_j(t) \sigma_y(t) + \frac{\Delta G^0}{\hbar} \sigma_y(t),$$

$$\dot{\sigma}_y(t) = -4b(t)\sigma_z(t) - \frac{2}{\hbar} \sum_j \gamma_j q_j(t) \sigma_x(t) - \frac{\Delta G^0}{\hbar} \sigma_x(t), \quad (3)$$

$$\dot{\sigma}_z(t) = 4b(t)\sigma_y(t),$$

and for the oscillators' variables,

$$\dot{q}_j(t) = \frac{p_j}{m_j}; \quad \dot{p}_j(t) = -m_j \omega_j^2 q_j(t) + \gamma_j \sigma_z(t). \quad (4)$$

The solvent-solute coupling, $\frac{2}{\hbar} \sum_j \gamma_j q_j(t)$, can be written as

$$\begin{aligned} \frac{2}{\hbar} \sum_j \gamma_j q_j(t) &= \frac{2}{\hbar} \left[\sum_j \gamma_j q_j(0) \cos \omega_j t + \frac{\gamma_j p_j(0)}{m_j \omega_j} \sin \omega_j t \right] \\ &+ \int_0^t ds \frac{E_r \omega_c}{\hbar} e^{-\omega_c(t-s)} \sigma_z(s). \end{aligned} \quad (5)$$

In writing Eq. (5) we have assumed an infinite number of oscillators for the solvent representation. That is, we have introduced the spectral density $J(\omega)$,³⁷

$$\sum_j \frac{\gamma_j^2}{m_j \omega_j^2} \cos \omega_j t \rightarrow \frac{2}{\pi} \int_{-\infty}^{\infty} d\omega \frac{J(\omega)}{\omega} \cos \omega t. \quad (6)$$

We shall assume that the coupling constants and the solvent frequencies are distributed with the Debye spectral density,³⁸

$$J(\omega) = \left(\frac{E_r}{2} \right) \frac{\omega \tau_c}{1 + (\omega \tau_c)^2} \theta(\omega). \quad (7)$$

With this assumption,

$$\sum_j \frac{\gamma_j^2}{m_j \omega_j^2} \cos \omega_j t \rightarrow \frac{E_r}{2} e^{-\omega_c t}, \quad (8)$$

and leads to the last term in Eq. (5). Note that Eq. (5) separates terms that depend on the oscillators initial conditions from those that do not. This separation will be important to the end of constructing an appropriate thermal ensemble. The following transformations of the coupling energy are useful:

$$\begin{aligned} \frac{2}{\hbar} \sum_j \gamma_j q_j(t) &= \frac{2}{\hbar} \left[\sum_j \gamma_j \left(q_j(0) - \frac{\gamma_j}{m_j \omega_j^2} \right) \cos \omega_j t \right. \\ &+ \left. \frac{\gamma_j p_j(0)}{m_j \omega_j} \sin \omega_j t \right] + \frac{2}{\hbar} \sum_j \frac{\gamma_j^2}{m_j \omega_j^2} \cos \omega_j t \\ &+ \int_0^t ds \frac{E_r \omega_c}{\hbar} e^{-\omega_c(t-s)} \sigma_z(s) \\ &= \frac{2}{\hbar} \left[\sum_j \gamma_j \left(q_j(0) - \frac{\gamma_j}{m_j \omega_j^2} \right) \cos \omega_j t \right. \\ &+ \left. \frac{\gamma_j p_j(0)}{m_j \omega_j} \sin \omega_j t \right] + \frac{E_r}{\hbar} e^{-\omega_c t} \\ &+ \int_0^t ds \frac{E_r \omega_c}{\hbar} e^{-\omega_c(t-s)} \sigma_z(s). \end{aligned} \quad (9)$$

By adding and subtracting the same quantity, Eq. (5) now can be re-cast as

$$\begin{aligned} \frac{2}{\hbar} \sum_j \gamma_j q_j(t) &= \eta(t) + \frac{E_r}{\hbar} (e^{-\omega_c t} - 1) \\ &+ \int_0^t ds \frac{E_r \omega_c}{\hbar} e^{-\omega_c(t-s)} \sigma_z(s) + \frac{E_r}{\hbar}. \end{aligned} \quad (10)$$

The last term of the previous formula can be combined with the standard free energy difference to yield $\hbar \omega_0 = \Delta G^0 + E_r$, the vertical electronic excitation energy between the (solvated) states $|0\rangle$ and $|1\rangle$. We have also introduced $\eta(t)$, which is given by

$$\begin{aligned} \eta(t) &= \frac{2}{\hbar} \left[\sum_j \gamma_j \left(q_j(0) - \frac{\gamma_j}{m_j \omega_j^2} \right) \cos \omega_j t \right. \\ &+ \left. \frac{\gamma_j p_j(0)}{m_j \omega_j} \sin \omega_j t \right]. \end{aligned} \quad (11)$$

As we shall see below, $\hbar \eta(t)$ is the appropriate energetic coupling to characterize an autonomous process. The properties of the solute only enter $\eta(t)$ through the (initial) displacement of the oscillators to the values $q_j(0) = \gamma_j / m_j \omega_j^2$ that represent their equilibration to the solute's $|0\rangle$ state.

Now define an interaction energy $\hbar \xi(t)$ according to

$$\begin{aligned} \xi(t) &= \eta(t) + \frac{E_r}{\hbar} (e^{-\omega_c t} - 1) \\ &+ \int_0^t ds \frac{E_r \omega_c}{\hbar} e^{-\omega_c(t-s)} \sigma_z(s). \end{aligned} \quad (12)$$

Besides the solute dependence of $\eta(t)$, $\xi(t)$ has the additional dependence on the history of the value of $\sigma_z(t)$, the Heisenberg operator for the solute population difference. The nonautonomous character of the solvent's energy evolution comes from the final two terms in Eq. (12). After these transformations we have the still exact Heisenberg equations of motion,

$$\begin{aligned} \dot{\sigma}_x(t) &= (\xi(t) + \omega_0) \sigma_y(t), \\ \dot{\sigma}_y(t) &= -4b(t) \sigma_z(t) - (\xi(t) + \omega_0) \sigma_x(t), \\ \dot{\sigma}_z(t) &= 4b(t) \sigma_y(t), \end{aligned} \quad (13)$$

with $\xi(t)$ given by Eq. (12) above.

The quantities of direct interest are the instantaneous population difference between the electronic states, $z(t)$, and the power absorbed by the solute from the external field, $\mathcal{P}(t)$, respectively, whose expectation values are

$$\langle z(t) \rangle = \text{Tr}(\rho(0) \sigma_z(t)) \quad (14)$$

and

$$\langle \mathcal{P}(t) \rangle = \text{Tr}(\rho(0) 2\hbar \dot{b}(t) \sigma_x(t)), \quad (15)$$

where the trace is over *all* the degrees of freedom, as indicated with the notation $\langle \dots \rangle$. Because the Hamiltonian is explicitly time dependent, due to the (classical) external field, we have written $\rho(0)$ in Eqs. (14) and (15) to empha-

size that the expectation values of the dynamical variables in the Heisenberg picture at time t are taken with the functional form of the initial density operator.

Before the external field is turned on, the solvent is equilibrated to the solute's initial state, $|0\rangle$. Thus, an appropriate initial ensemble is equilibrium of the solvent conditional on this solute state:

$$\rho(0) \propto \exp \left\{ -\beta \left[\sum_j \frac{p_j^2}{2m_j} + \frac{1}{2} m_j \omega_j^2 \left(q_j - \frac{\gamma_j}{m_j \omega_j^2} \sigma_z \right)^2 \right] \right\} \times (\hat{1} + \sigma_z). \quad (16)$$

To make progress with this nonlinearly coupled quantum mechanical system, one needs to introduce simplifying assumptions. We shall assume that the solvent oscillators may be treated classically. The use of a classical bath is appropriate for $\beta \hbar \omega_m < 1$, where ω_m is a characteristic solvent frequency. For polar solvents, where the relevant modes that couple to a charged solute are the orientational dipoles of the solvent, the characteristic frequencies are less than 100 cm^{-1} , and the use of a classical bath is a good approximation at conventional temperatures.³³ With the initial ensemble considered here, it is straightforward to show that the Hamiltonian version of $\eta(t)$ is equivalent to a Gaussian stochastic process of zero average and exponential correlation function,³⁹⁻⁴¹

$$\langle \eta(t) \eta(0) \rangle = K(t) = \Delta^2 e^{-t/\tau_c}, \quad (17)$$

characterized by the strength $\Delta = \sqrt{2E_r k_B T / \hbar^2}$, and correlation time $\tau_c = 1/\omega_c$. That $\eta(t)$ has zero average is due to our having defined it as the fluctuation away from the value E_r . The above stationary, Markovian, and Gaussian process is known as an Ornstein-Uhlenbeck (OU) process,⁴² and can be generated by the solution of the equation

$$\dot{\eta}(t) = -\omega_c \eta(t) + w(t), \quad (18)$$

where $w(t)$ is a zero-average white noise with correlation function $\langle w(t)w(s) \rangle = 2\Delta^2 \omega_c \delta(t-s)$. The initial value $\eta(0) = \eta$ of $\eta(t)$ is distributed according to the Gaussian distribution,

$$W(\eta) = \frac{1}{\sqrt{2\pi\Delta^2}} e^{-\eta^2/2\Delta^2}. \quad (19)$$

This expression is the classical analog of the initial distribution given in Eq. (16). It describes the classical solvent equilibrated to the initial solute state, $|0\rangle$. The formulation of the stochastic process $\eta(t)$ as a differential equation has proved to be very useful in our approach to SFS. For obtaining the new results that require a solution with the stochastic process $\xi(t)$, it will be essential.

Another approximation we shall use is to assume that $\xi(t)$ depends on the expectation value of $\sigma_z(s)$. This time dependent mean field approximation has been used repeatedly in the literature to analyze the influence of classical variables on the tunneling of quantum objects.⁴³ With this assumption, quantum fluctuations in spin space that might be important at low temperatures or very strong bath-spin cou-

plings are neglected. The analysis of the validity of this assumption in the context of strong field spectroscopy will be presented elsewhere.⁴⁴

Denote the initial state matrix elements of the components of the spin operators as $z(t) = \langle 0 | \sigma_z(t) | 0 \rangle$, $x(t) = \langle 0 | \sigma_x(t) | 0 \rangle$, and $y(t) = \langle 0 | \sigma_y(t) | 0 \rangle$. Averaging the set, Eqs. (12) and (13), with the initial oscillator distribution in Eq. (16), and taking the trace over only the spin variables, yields the stochastic differential equations,

$$\begin{aligned} \dot{x}(t) &= [\omega_0 + \xi(t)]y(t), \\ \dot{y}(t) &= -[\omega_0 + \xi(t)]x(t) - 4b(t)z(t), \\ \dot{z}(t) &= 4b(t)y(t), \end{aligned} \quad (20)$$

where $\xi(t)$ is a stochastic variable given by

$$\begin{aligned} \xi(t) &= \eta(t) + \frac{E_r}{\hbar} (e^{-\omega_c t} - 1) + \int_0^t ds \frac{E_r \omega_c}{\hbar} e^{-\omega_c(t-s)} z(s) \\ &= \eta(t) + \int_0^t ds \frac{E_r \omega_c}{\hbar} e^{-\omega_c(t-s)} [z(s) - 1]. \end{aligned} \quad (21)$$

The nonautonomous character of the solvent evolution is evident in Eq. (21). The stochastic variable $\xi(t)$ depends on the solute population difference $z(t)$ in a convolution form with the solvent's relaxation function $e^{-\omega_c t}$. It is worth noticing that we get a closed set of equations for the indicated matrix elements of the Pauli operators. This is a consequence of assuming that $\xi(t)$ depends only on $z(s)$ and not on the full Pauli matrix. With these approximations, the power absorbed also turns out to be a stochastic function of time,

$$P(t) = 2\hbar \dot{b}(t)x(t). \quad (22)$$

Before analyzing the implications of Eqs. (20) and (21), we shall indicate how these equations of motion reduce to those that we previously obtained. If the external field is sufficiently weak that $z(t) \approx 1$ during a large time interval of interest, then Eq. (21)'s second equality shows that $\xi(t)$ is just the OU process $\eta(t)$. The stochastic process representing the solvent dynamics is now independent of the spin dynamics. All the consequences of LRT, conventionally obtained by the use of the Golden Rule of time dependent perturbation theory, can also be obtained from Eq. (21).^{29,30} Note that this conclusion is independent of the relative sizes of E_r and $\hbar\Delta$. For SFS, where $z(t)$ does change significantly, if $\Delta > E_r/\hbar$, then the last term on the rhs of the second equality in Eq. (21) can also be neglected with respect to the first one and once more we go back to an autonomous bath. The demonstration of this result relies on estimating the sizes of the terms that contribute to Eq. (21). The first term is of order Δ . The second is of order E_r/\hbar . If we assert that $z(t)$ oscillates with a frequency that is essentially the Rabi frequency, $2b_0$, then the integral in the third term may be evaluated. For large $b_0\tau_c$, the ratios of the second and third terms to the first term then are, respectively, $\sqrt{E_r/kT}$ and $\sqrt{E_r/kT}/(b_0\tau_c)$. For $E_r/\hbar\Delta = \sqrt{E_r/2kT} < 1$ and for $b_0\tau_c > 1$, as is readily achieved for the strong fields considered here, the second and third terms may be neglected relative to the first term in Eq. (21). Thus, in both these

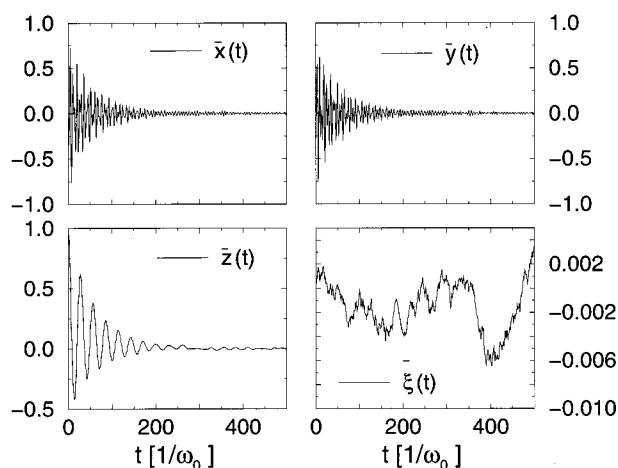


FIG. 1. The averages $\bar{x}(t)$, $\bar{y}(t)$, $\bar{z}(t)$, $\bar{\xi}(t)$ for $E_r=0$, $b_0=0.1$, $\Delta=0.15$, $\omega_c=0.015$, and $\Omega=\omega_0=1.0$.

cases, LRT and SFS with $\Delta > E_r/\hbar$, the bath behavior is autonomous and the task of obtaining equations of motion for the averages over the stochastic process can be achieved under some suitable approximations.^{29,30}

III. ANALYSIS OF THE NONAUTONOMOUS EQUATIONS OF MOTION

The nonautonomous system of equations of motion in Eqs. (20) and (21) is much more difficult to analyze than the autonomous equations. Even for the autonomous system, the analytic scheme we developed is only qualitatively accurate for slow modulation ($\Delta\tau_c > 1$), and the analysis still required some numerical calculations. Fortunately, the stochastic methods we⁴⁵ and others⁴⁶ have developed to solve stochastic differential equations of the autonomous variety can be adapted to the nonautonomous equations. Toward this goal, we first recast the integral equation for $\xi(t)$ as a differential equation. Taking time derivatives in Eq. (21) produces

$$\dot{\xi}(t) = -\omega_c \xi(t) + w(t) + \frac{E_r \omega_c}{\hbar} (z(t) - 1). \quad (23)$$

This last equation together with Eqs. (20) comprise a set of stochastic equations that are to be solved with the initial conditions $x(0)=y(0)=0, z(0)=1$ and $\xi(0)=\eta(0)$ drawn from the Gaussian distribution given in Eq. (19). To integrate the set of equations, we have used a stochastic Runge–Kutta algorithm of second order in the noise and the deterministic parts.⁴⁶ For each initial value of $\xi(0)$, Eqs. (20) and (23) are solved for a realization of the white noise $w(t)$. The scheme is repeated for other $\xi(0)$ values drawn from the Gaussian distribution in Eq. (19). The number of initial conditions generated to get reliable statistics is chosen accordingly to the width, Δ , of that distribution. We have constructed histograms for the generated initial distribution of η values to compare with the theoretical expression in Eq. (19). Taking into account the definition of the white noise strength in terms of Δ and ω_c , the generation of as many white noise realizations as of initial conditions also guarantees that, except if ω_c is very large, we have a reliable numerical ap-

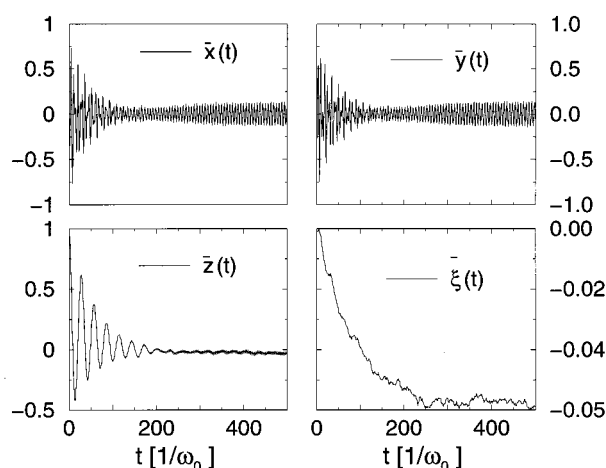


FIG. 2. The averages $\bar{x}(t)$, $\bar{y}(t)$, $\bar{z}(t)$, $\bar{\xi}(t)$ as in Fig. 1 but for $E_r=0.05$.

proximation of the white noise. The time evolution of the averages, denoted by $\overline{\cdots}(t)$, is obtained by summing over the white noise realizations that are generated from all the initial conditions.

In order to demonstrate the character of the nonautonomous predictions, and how they differ from those of the autonomous equations of motion, it is useful to first focus on the behaviors of $\bar{x}(t)$, $\bar{y}(t)$, and $\bar{z}(t)$. After discussing this behavior, we shall investigate the average power absorbed, $\bar{\mathcal{P}}(t)$. Figs. 1–4 display $\bar{x}(t)$, $\bar{y}(t)$, $\bar{z}(t)$, and $\bar{\xi}(t)$ for a variety of E_r values. The parameter values are chosen to be representative of a polar solvent at conventional temperatures (cf. Sec. VI), where a classical treatment of the bath is appropriate. All the figures use parameter values that are scaled by the transition frequency ω_0 . We have set $\omega_0=1$, so that different energetic scales of, e.g., reorganization energy can be compared on a common basis. Features of these plots, and others that we have generated that are of interest, are the following. For large times, $\bar{z}(t)$ oscillates around 0 if $E_r \ll \hbar\Delta$ and around a nonzero value if $E_r \geq \hbar\Delta$. The frequency of those oscillations is $2\omega_0$. When $E_r \ll \hbar\Delta$ these

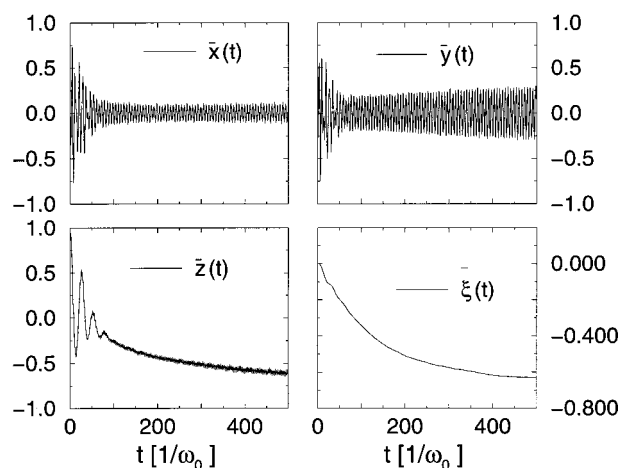


FIG. 3. The averages $\bar{x}(t)$, $\bar{y}(t)$, $\bar{z}(t)$, $\bar{\xi}(t)$ as in Fig. 1 but for $E_r=0.4$.

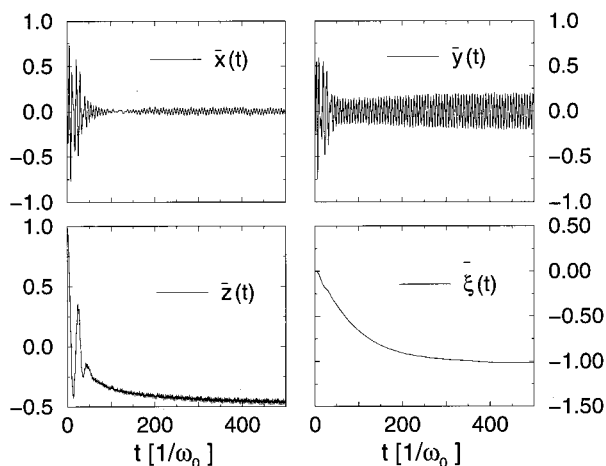


FIG. 4. The averages $\bar{x}(t)$, $\bar{y}(t)$, $\bar{z}(t)$, $\bar{\xi}(t)$ as in Fig. 1 but for $E_r=0.7$.

fast oscillations are hardly noticeable as they are of a much smaller amplitude than the slower Rabi oscillations around zero. These fast oscillations are more clearly seen when $E_r \geq \hbar\Delta$. The center of those oscillations is more negative as b_0 is increased. Keeping the field strength large and fixed, and varying E_r , one observes that the shift of the center of oscillations towards negative values is not monotonous with E_r . For instance, if $b_0=0.1$ the center shifts from $\bar{z}_0 \approx -0.1$ for $E_r=0.1$, to $\bar{z}_0 \approx -0.6$ for $E_r=0.4$, to $\bar{z}_0 \approx -0.45$ for $E_r=0.7$. (The notation $\bar{\alpha}_0$, with α any relevant variable, designates the long-time average over the oscillatory behavior.) For large times, $\bar{\xi}(t)$ decays to almost zero if $E_r \ll \hbar\Delta$ and to a nonzero negative value if $E_r \geq \hbar\Delta$. With regard to the other spin components, $\bar{x}(t)$ and $\bar{y}(t)$ show oscillations around zero for long times. The frequency of the oscillations is ω_0 , and their amplitudes depend on b_0 and E_r . For a given E_r , the amplitude of the oscillations increases with b_0 . For a fixed value of the field strength, the amplitude of the $\bar{x}(t)$ oscillations first increases as E_r increases from zero to a certain value, and then the amplitude decreases as E_r is further increased.

Turning now to the average power, $\bar{\mathcal{P}}(t)$, obtained by the stochastic simulation of Eq. (15), it proves useful to analyze the power spectrum, obtained from the Fourier transform of $\bar{\mathcal{P}}(t)$. The power spectrum $|\bar{\mathcal{P}}(\omega)|^2$, with ω the transform parameter, is shown in Fig. 5. There are several peaks in the spectrum: a low frequency large peak and three peaks at higher frequencies. The high-frequency peaks appear because we are not cycle averaging over the external field frequency, Ω . The positions of the peaks are controlled essentially by b_0 , except for the one at 2Ω . The asymmetry in the heights of the two side peaks around the one at 2Ω is more pronounced as E_r increases. The distance between them is basically given by $4b_0$. The width of all the peaks also depends on E_r . The properties of the low-frequency peaks and the two side ones can be obtained from the approximate expressions that we obtained before in the case of an autonomous bath, where $E_r < \hbar\Delta$.^{29,30} When the medium feels the feedback of the spin dynamics, our approximate

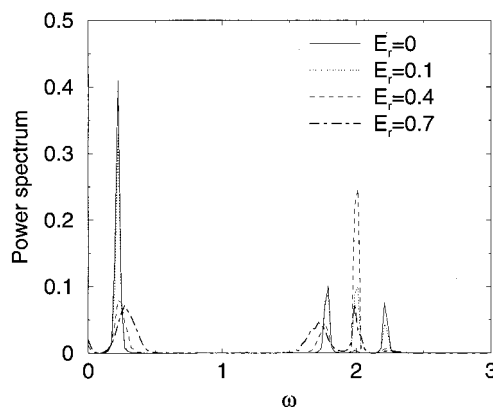


FIG. 5. Power spectrum of the power absorbed for the parameter values $b_0=0.1$, $\omega_0=\Omega=1.0$, $\Delta=0.15$, $\omega_c=0.015$, and several values of the reorganization energy, E_r . As E_r increases, there are changes in the relative intensities of the peaks, but their positions and widths are quite similar, at least for small E_r .

expressions lose their validity. Still, the locations of the peaks are not substantially altered, and their widths increase modestly with respect to the autonomous case. That the autonomous and nonautonomous power spectra are quite similar is a useful observation. We have recently shown that SFS can be used to circumvent inhomogeneous broadening effects.⁴⁷ That is, the dissipative information contained in the widths of these power spectra is still related to the homogeneous parameters of the problem. For example, for fast modulation, the width of the power spectrum is still given by the homogeneous dissipation parameter, $\Delta^2\tau_c$. These numerical findings illustrate that there are effects on the spectrum that reflect the autonomous and nonautonomous regimes. Nevertheless, the effects are not too significant unless E_r is very large, and the autonomous analysis that we previously obtained can be a guide in interpreting the new results.

The key feature that $\bar{z}(t)$ is negative and substantially different from zero at long times for $E_r > \hbar\Delta$ [and when b_0 is sufficiently large as to drive $\bar{z}(t)$ significantly] is a manifestation of the dynamical feedback from the spin to the bath as represented by the $\xi(t)$ stochastic process. If the dynamics are autonomous, the dephasing from the bath is symmetrically disposed. That is, the modulation of the transition frequency of the solute by the solvent is as likely to increase as it is to decrease. Consequently, the phase mixing responsible for $\bar{z}(t)$'s damping will lead to equality of the population of the two states. Indeed, at least for fast modulation where an analytic approach was feasible, we were able to show that $\bar{z}(t)$ obeyed a damped harmonic oscillator equation of motion.²⁹ The nonautonomous dynamics is radically different. To explore this difference, we now discuss the case of weak noise, where the noise term is negligible in Eq. (21).

IV. THE DETERMINISTIC LIMIT

The qualitative features of the stochastic equation solutions when nonautonomous behavior is important are already evident in a set of deterministic equations obtained by dropping the white noise term in the $\xi(t)$ evolution equation. In particular, the long-time behavior can be clarified by solving

these deterministic equations. An estimate of the conditions under which the noise term in Eq. (23) can be neglected is the following: Using the definition $\tilde{t} = \omega_c t$ in Eq. (21) produces

$$\dot{\xi}(\tilde{t}) = -\xi(\tilde{t}) + \frac{\sqrt{2D\omega_c}}{\omega_c} \chi(\tilde{t}) + \frac{E_r}{\hbar} (z(\tilde{t}) - 1), \quad (24)$$

where $\langle \chi(\tilde{t})\chi \rangle = \delta(\tilde{t})$. Here D is the strength of the white noise that is obtained from the other parameters of the bath as $D = \Delta^2 \omega_c$. Then, the white noise term is negligible with respect to the third term if

$$\sqrt{\frac{D}{\omega_c}} < \frac{E_r}{\hbar} \quad \text{or} \quad \Delta < \frac{E_r}{\hbar}.$$

This condition indicates when the effect of the reorganization energy is more important than the stochastic nature of the bath, these fluctuations being characterized by the strength of the noise. The deterministic limit is favored when the $\xi(t)$ process is strongly nonautonomous. In the opposite extreme, the autonomous process has no such limiting, deterministic behavior because, if the noise is neglected in the autonomous process, $\eta(t)$ is zero, and the spin only exhibits Rabi oscillations.

The deterministic approximation to the equations of motion of Eqs. (20) and (23) is

$$\begin{aligned} \dot{x}(t) &= [\omega_0 + \xi(t)]y(t), \\ \dot{y}(t) &= -[\omega_0 + \xi(t)]x(t) - 4b(t)z(t), \\ \dot{z}(t) &= 4b(t)y(t), \\ \dot{\xi}(t) &= -\omega_c \xi(t) + \frac{E_r \omega_c}{\hbar} (z(t) - 1). \end{aligned} \quad (25)$$

It is readily verified that $x^2(t) + y^2(t) + z^2(t)$ is constant in time. Even though the noise has been neglected, there is still relaxation in the dynamics of $\xi(t)$ due to the $-\omega_c$ term on the right hand side of its evolution equation. This term makes the bath dissipate any energy transferred to it from the spin through the population difference. Even with this simplification to a deterministic process, Eq. (25) cannot be solved analytically. The numerical solution of the deterministic equations of motion in Eq. (25) for a few parameter values is shown in Fig. 6. Additional data is presented in Table I.

Based on an extensive set of numerical solutions, we observe the following features that will aid in understanding the deterministic behavior: After a transient time, $x(t)$ and $y(t)$ oscillate with frequency ω_0 and amplitudes that decrease as E_r increases. The out-of-phase (with respect to the external field) component, $y(t)$, always oscillates around zero, but the center of oscillations of $x(t)$ shifts from zero to some other value as E_r increases. For example, when we take $b_0 = 0.15$, $\omega_c = 0.2$ and $E_r \leq 0.7$, corresponding to strong nonautonomous behavior, $x(t)$ eventually oscillates around a nonzero value with very small amplitude. At long times, $z(t)$ oscillates with frequency $2\omega_0$ and an amplitude that decreases as E_r increases. The center of oscillations, call it z_0 , moves towards a more negative value as E_r increases. Once E_r is large enough that the alluded shift of $x(t)$ takes place,

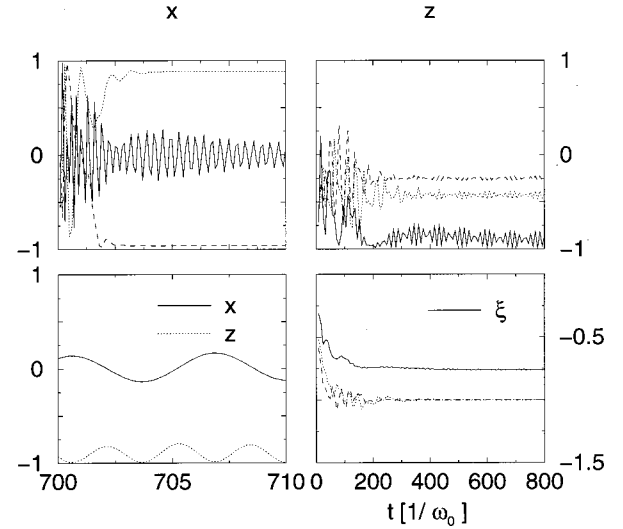


FIG. 6. Deterministic values of x , z , ξ for $b_0 = 0.15$, $\omega_c = 0.2$, $\omega_0 = \Omega = 1.0$ and $E_r = 0.4$ (solid line), $E_r = 0.7$ (dotted line), and $E_r = 0.8$ (dashed line). The plots do not show the details of the large frequency oscillations. The lowest left panel shows the large frequency oscillations of x , z ($E_r = 0.4$) for long times.

the amplitude of the $z(t)$ oscillations is very small. At long times, $\xi(t)$ oscillates with frequency $2\omega_0$ and very small amplitude around a negative value ξ_0 that decreases as E_r increases. At long times $\xi_0 \approx E_r(z_0 - 1)$. Once E_r is sufficiently large, whereby the center of oscillation of $x(t)$ shifts from zero to some other value, $\xi_0 = -1$.

Before analyzing the implications of the above behavior, let us consider an approximation that one might think would be useful but, in fact, leads to incorrect conclusions. Nevertheless, it is quite instructive. The integral form of the evolution of $\xi(t)$ given in Eq. (21), and the fact that $\xi_0 \approx E_r(z_0 - 1)$ holds after a transient time, as evident in Figs. 1–4 and 6, suggest that a time local version of this equation would be useful. The local relation,

$$\xi(t) = (1 - e^{-\omega_c t}) E_r [z(t) - 1], \quad (26)$$

follows from the $\xi(t)$ equation in Eq. (21), if we assume that $z(t)$'s behavior is slow relative to that of $\exp(-\omega_c t)$. Using this local relation in the spin equations of motion of Eq. (25) the solution is (off-resonant) Rabi oscillations. Even if one were to assert that the behavior of $\xi(t)$ is a damped oscillation, and used this in the spin equations of Eq. (25), Rabi

TABLE I. Results of deterministic equations for $b_0 = 0.15$; $\omega_c = 0.2$; $\omega_0 = \Omega = 1.0$.^a

E_r	x_0	A_x	y_0	A_y	z_0	A_z	ξ_0	A_ξ
0.05	0	0.9	0	1	-0.1	0.1	-0.05	~ 0
0.1	0	0.8	0	0.95	-0.38	0.1	-0.14	~ 0
0.2	0	0.5	0	0.8	-0.7	0.1	-0.35	~ 0
0.4	0	0.1	0	0.6	-0.9	0.1	-0.76	~ 0
0.7	0.8	0	0	0.2	-0.4	0.05	-1	~ 0
0.8	-0.95	0	0	0.15	-0.25	0.05	-1	~ 0

^a A_i and i_0 denote amplitudes and center of oscillations of the $i = x, y, z, \xi$ variables.

oscillations would result. Thus, in order to obtain the correct damped oscillatory solution exhibited in Figs. 1–4 and 6, it is essential to incorporate the time nonlocal character of $\xi(t)$.

The energy of interaction between the solvent and solute, $\xi(t)$, decays because it is the convolution of the solvent's attempt to decay toward equilibrium according to $\exp(-\omega_c t)$ and the population difference $z(t)$. The solvent is continuously trying to adjust to $z(t)$, and $z(t)$ is being driven by the external field at a frequency connected to the instantaneous state of the solvent. It is this convolution structure that then leads to the observed decaying behavior. The nonautonomous character of the connection between $\xi(t)$ and $z(t)$'s dynamics then shows that if $\xi(t)$ decays, so must $z(t)$. Therefore, $z(t)$ must exhibit both oscillation and decay.

The numerical solutions show that $z(t)$ approaches a steady value for long times. We can identify a steady state behavior from the equations of motion by introducing cycle-averaged values of $x(t)$, $y(t)$, $z(t)$, and $\xi(t)$ according to \bar{x}^c , \bar{y}^c , \bar{z}^c , and $\bar{\xi}^c$. The average is carried out over the period of the external field frequency Ω . If E_r is sufficiently large then, as noted above, the scale of oscillation in z and ξ is small. This permits us to obtain the steady state, cycle-averaged version of Eq. (25) as

$$\begin{aligned}\dot{\bar{x}}^c &= 0 = \omega_0 \bar{y}^c + \bar{\xi} \bar{y}^c \approx \bar{\xi}^c \bar{y}^c, \\ \dot{\bar{y}}^c &= 0 = -[\omega_0 \bar{x}^c + \bar{\xi} \bar{x}^c] - 4\overline{b(t)z}^c \approx -\omega_0 \bar{x}^c - \bar{\xi}^c \bar{x}^c, \\ \dot{\bar{z}}^c &= 0 = 4\overline{b(t)y}^c, \\ \dot{\bar{\xi}}^c &= 0 = -\omega_c \bar{\xi}^c + \frac{E_r \omega_c}{\hbar} (\bar{z}^c - 1).\end{aligned}\quad (27)$$

From the fact that $\bar{y}^c = 0$, the $\dot{\bar{x}}^c$ equation is satisfied. Since $b(t)$ is out of phase with $y(t)$ the $\dot{\bar{z}}^c = 0$ equation is satisfied. If, as assumed, $z(t)$ is almost constant, the $\dot{\bar{y}}^c$ equation then gives the key result,

$$\bar{\xi}^c = -\omega_0. \quad (28)$$

Finally, according to the $\dot{\bar{\xi}}^c = 0$ equation, \bar{z}^c exists and, with the use of Eq. (28), its value is

$$\bar{z}^c = 1 - \frac{\hbar \omega_0}{E_r}. \quad (29)$$

For sufficiently large E_r , as in Fig. 6, this behavior is verified. If we consider that $E_r < \hbar \omega_0$, as a normal regime of behavior in optical spectroscopy, then $\bar{z}^c < 0$ follows, and corresponds to a partial population inversion.

The analysis leading to Eq. (28) does not hold when E_r is smaller. The oscillations are too large to permit separating the cycle-averages that appear in Eq. (27) into products of cycle averages. Nonetheless, that cycle-averaged steady states are possible is evident from the analysis. That $\bar{z}^c \neq 0$ is not surprising since the nonautonomous equations of motion are nonresonant in character. For the nonstochastic version of the autonomous equations of motion, the cycle average behavior of $z(t)$ will also be nonzero for off resonance. What

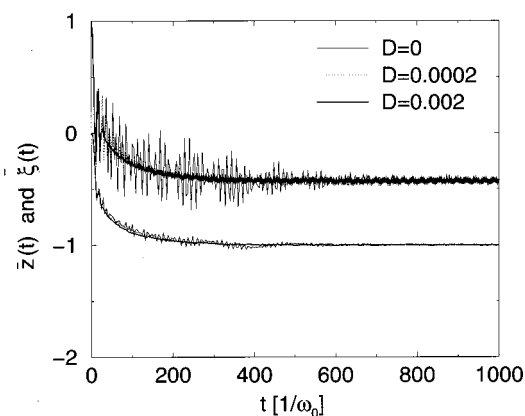


FIG. 7. $\bar{\xi}(t)$ and $\bar{z}(t)$ for $D=0.0, 0.0002$, and 0.002 , with $E_r=0.7$, $b_0=0.1$, $\omega_c=0.2$, and $\Omega=\omega_0=1.0$. The damping of the initial oscillations for $D \neq 0.0$ is evident. The long-time deterministic and stochastic behavior is similar, emphasizing the decisive role of the nonautonomous feedback.

is completely different is that $z(t)$ has a damped oscillatory behavior for $E_r > 0$, while for $E_r = 0$, $z(t)$ will oscillate with the same amplitude for all time. The convolution structure of the interaction energy $\hbar \xi(t)$ provides a damping mechanism for $\xi(t)$, and the feedback between ξ and z “slaves” the spin to the bath, so $z(t)$ also decays to produce a cycle-averaged steady state. Proving that $\bar{z}^c < 0$ in general does not seem possible, though the data presented in Fig. 6 and Table I do show that it is true. Interestingly, the \bar{z}^c behavior is not monotonic with increasing E_r , but rather exhibits a maximum $\bar{z}^c \approx -1$ at intermediate E_r values.

Let us now compare the results of the deterministic and stochastic solutions of the equations of motion. Figure 7 shows that as the noise increases from zero, for the deterministic case, to $D=0.0002$ to $D=0.002$, the behavior of the stochastic averages is a damped version of the deterministic. Note that D does not have to be particularly large in order to suppress the initial oscillations in $\bar{\xi}(t)$. The behavior of $\bar{z}(t)$ is similar. The long-time behavior of the three curves is quite similar; thus emphasizing again that the origin of the nonzero value of \bar{z}^c is the nonautonomous average behavior. That is, the fluctuations are not very important to this long-time behavior.

V. POPULATION CONTROL

Controlling outcomes of various chemical processes is a natural goal when external fields are applied to matter.^{14–17} Within the context of tunneling processes described as two-level^{18–20} or few-level systems,^{21,22} most work has been concentrated on the gas phase. We have studied the role of a solvent in attempts at control of the fate of tunneling reactions and, not surprisingly, the solvent fluctuations tend to destroy the ability to control the populations.^{40,45} In view of the results of the previous section, where the deterministic solution is close to the stochastic one, it is natural to see if the population difference $\bar{z}(t)$ can be controlled by the use of an appropriate external field. All the above simulations have kept the field on for times long compared with the relaxation

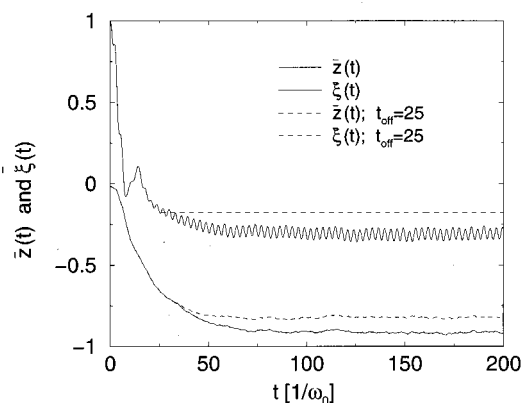


FIG. 8. $\bar{z}(t)$ and $\bar{\xi}(t)$ with the field on for times long compared with the system relaxation time and cut-off at $t_{\text{off}}=25.0$, for $E_r=0.7$, $\omega_c=0.1$, $\Delta=0.387$, $b_0=0.15$, and $\Omega=\omega_0=1.0$. When the external field is cut-off, the evolution of $\bar{z}(t)$ stops completely and $\bar{\xi}(t)$ essentially stops evolving, as proved in Sec. V.

time of the system. In Fig. 8 we show the consequences of turning off the field before relaxation is complete. It is evident that as soon as the field is off, both $\bar{z}(t)$ and $\bar{\xi}(t)$ cease their time evolution at the value they had when the field goes off, t_{off} . This behavior is readily obtained from the deterministic equations of motion in Eq. (25). When the field is turned off [$b(t)=0$], $\dot{z}=0$ and $z(t)=z(t_{\text{off}})=z_{\text{off}}$, for $t>t_{\text{off}}$. Then the $\xi(t)$ equation becomes

$$\xi(t)=\xi(t_{\text{off}})=\xi_{\text{off}}=\frac{E_r}{\hbar}(1-e^{-\omega_c t})(z_{\text{off}}-1)\approx\frac{E_r}{\hbar}(z_{\text{off}}-1). \quad (30)$$

The last relation holds for $t\gg 1/\omega_c$, which is a short time on the scale of t_{off} . Once ξ is constant, the spin equations of motion for $x(t)$ and $y(t)$ correspond to harmonic oscillators of frequency $\omega_0+\xi_{\text{off}}$. That $\xi(t)$ does not cut off sharply at t_{off} just reflects the fact that t_{off} is not much greater than $1/\omega_c$ for the parameters used to generate Fig. 8 ($1/\omega_c=10.0$ and $t_{\text{off}}=25.0$). For the stochastic equations of motion in Eqs. (20) and (21), a similar analysis can be carried out for each realization of the stochastic trajectory with a fixed initial value $\xi(0)$. Again for times $t\gg 1/\omega_c$, it leads to the same $\xi(t_{\text{off}})=(E_r/\hbar)(z_{\text{off}}-1)$ relation and this will be the case for all $\xi(0)$ values. Thus, the same behavior as for the deterministic case will result for the stochastic solution. These results suggest that if t_{off} is chosen before $z(t)$ reaches its limiting value, then the population can be controlled by the choice of t_{off} . The stochastic equations of motion have the advantage over the deterministic ones in that there is much more damping of the initial oscillations for the stochastic; therefore, the population can be better controlled in the (realistic) stochastic situation. The combination of fluctuations and nonautonomous behavior is responsible for the ability to select a target population.

VI. CONCLUDING REMARKS

The parameter values used to generate Figs. 1–6 were chosen to be representative of a polar solvent. For example,

if the transition frequency ω_0 is taken as 1000 cm^{-1} , then $\Delta=150\text{ cm}^{-1}$, and E_r ranges from $100\text{--}700\text{ cm}^{-1}$ (scaled units $E_r=0.1\text{--}0.7$). This choice of E_r values, spanning the autonomous to nonautonomous range, is typical of polar solvents. The relaxation time τ_c is about 350 fs, which is representative of fast polar solvent relaxation. Notice that once the value of Δ is fixed, varying the value of E_r implies a change in the temperature T . With the figures quoted above, the temperatures are still larger than $\hbar\omega_c$ so that the classical approximation for the bath intrinsic fluctuations remains valid. The results presented in Figs. 1–6 are representative of what is obtained, so slower relaxation times and changes in E_r do not alter our conclusions. Increasing ω_0 to $10,000\text{ cm}^{-1}$ scales Δ up to 1500 cm^{-1} , and even here $E_r>\Delta$ is not unphysical, as reorganization energies of this magnitude are readily achieved in polar solvents when the electronic structures of the ground and excited states are substantially different.

In SFS there is a clear distinction between the dynamics of the solute and solvent demarcated by the condition E_r less than or greater than $\hbar\Delta$. In the former case, the evolution of the solvent is autonomous, while in the latter it is nonautonomous. The initial condition of bath equilibrium conditional on the initial solute state, $|0\rangle$, is the sole influence of the solute on the solvent in the autonomous evolution. When the solute population is hardly changing, as assumed in LRT, the initial condition $z(0)=1$ is approximately true for all relevant times, and the autonomous equations of motion should hold for all relative values of E_r and $\hbar\Delta$. In SFS, where the population difference is being driven away from $z(0)=1$ by the action of the (strong) external field, the analysis in Sec. II shows that for $E_r<\hbar\Delta$, autonomous dynamics still is a good approximation; the fluctuations dominate the bath evolution. Conversely, when $E_r>\hbar\Delta$, the nonautonomous character is important, and leads to the new behavior.

The prime manifestation of the nonautonomous behavior is the relaxation of $\bar{z}(t)$ to a negative long-time average value. The population is being inverted in this sense in contrast with the autonomous behavior where the populations of the two states equalize. The way this comes about is quite roundabout, as evidenced by the requirement of a nonlocal relation between $z(t)$ and $\xi(t)$ that is given in Eq. (21). As noted in Sec. IV, if a local-in-time relation between $z(t)$ and $\xi(t)$ is assumed, there will be only oscillatory behavior. And the oscillation frequency can be thought of as analogous to what would be obtained for an off-resonant Rabi oscillator. The convolution structure in Eq. (21) represents the delay in the response of the energetic coupling $\hbar\xi(t)$ to the constantly changing population difference, $\bar{z}(t)$. The population difference is always being driven by the external field; thus $\xi(t)$ must always try to re-equilibrate to the instantaneous value of $z(t)$, with the solvent response time measured by ω_c .

The analysis of what we referred to in Sec. IV as the deterministic equations of motion, Eq. (25), shows that the above-noted behavior is evident even when the fluctuations, with strength measured by Δ , are weak compared with the average value E_r . Note that in the $\eta(t)$ stochastic process,

the average is zero because we have defined η as a fluctuation away from E_r . This is the most useful choice when the initial condition is the solvent equilibrated to state $|0\rangle$. The long-time behavior of the system is dominated by the non-autonomous character of the equations of motion, versus their stochastic character.

The procedure used in Sec. II to separate the interaction energy $\hbar\xi(t)$ into parts that depend on the bath initial coordinates and momenta, relative to the solute's initial state, as in Eqs. (12) and (11), is responsible for the relatively simple form of the equations of motion in Eq. (13). Combined with the bath initial condition in Eq. (16), describing the solvent equilibrated to the solute's $|0\rangle$ state, this formulation is the most direct one to deal with the population evolution as driven by the external field and by the coupled spin and bath dynamics. With the introduction of a classical treatment of the solvent and the mean-field approximation for the spin dynamics in the bath evolution, Eqs. (20) and (23) show that a stochastic process formulation is still feasible even for the nonautonomous dynamics.

From a computational viewpoint, the stochastic formulation is much easier to deal with than the Hamiltonian one. Integrating the four equations of motion is efficiently carried out by the method of generating a white noise realization for each initial $\xi=\eta$ value, and adding the results from trajectories generated with the Gaussian distribution of η 's. Analytically, the $\xi(t)$ process is much harder to deal with than the stationary, Markovian (so, exponentially correlated) and Gaussian $\eta(t)$ process. Indeed, $\xi(t)$ is not a stationary process; $\xi(t_1)\xi(t_2)\neq\xi(t_1+\tau)\xi(t_2+\tau)$, nor is its correlation function exponential. The feedback from the spin variable precludes a simple description of the stochastic properties of $\xi(t)$, and this prevents an analytic approach based on stochastic process theory.

ACKNOWLEDGMENTS

Support by NATO (R.I.C. and M.M.), the Center for Fundamental Materials Research at Michigan State University (R.I.C. and M.M.), and the Dirección General de Enseñanza Superior of Spain (Project No. PB95-0536) and the Junta de Andalucía (M.M. and C.D.) is gratefully acknowledged.

¹W. E. Moerner, in *Persistent Spectral Hole Burning: Science and Applications* (Springer-Verlag, Berlin, 1988).

²S. Mukamel, *Principles of Nonlinear Optical Spectroscopy* (Oxford University Press, New York, 1995).

³J. L. Skinner and W. E. Moerner, *J. Phys. Chem.* **100**, 13251 (1996).

⁴G. Fleming and M. Cho, *Annu. Rev. Phys. Chem.* **47**, 109 (1996).

⁵W. P. de Boeij, M. S. Pshenichnikov, and D. A. Wiersma, *J. Phys. Chem.* **100**, 11806 (1996).

⁶A. B. Myers, *Annu. Rev. Phys. Chem.* **49**, 267 (1998).

⁷P. Cong, Y. J. Yan, H. P. Deuel, and J. D. Simon, *J. Chem. Phys.* **100**, 7855 (1994).

⁸T.-Y. Yang, P. Vöhringer, D. C. Arnett, and N. F. Scherer, *J. Chem. Phys.* **103**, 8346 (1995).

⁹M. Cho, J.-Y. Yu, T. Joo, Y. Nagasawa, S. A. Passino, and G. R. Fleming, *J. Phys. Chem.* **100**, 11944 (1996).

¹⁰A. M. Stoneham, *Rev. Mod. Phys.* **41**, 82 (1969).

¹¹L. R. Narasimhan, K. A. Littau, D. W. Pack, Y. S. Bai, A. Elschner, and M. D. Fayer, *Chem. Rev.* **90**, 439 (1990).

¹²S. G. Boxer, D. S. Gottfried, D. J. Lockhart, and T. R. Middendorf, *J. Chem. Phys.* **86**, 2439 (1987).

¹³D. T. Leeson, O. Berg, and D. A. Wiersma, *J. Phys. Chem.* **98**, 3913 (1994).

¹⁴S.-I. Chu, *Adv. Chem. Phys.* **73**, 739 (1986).

¹⁵W. Domcke, P. Hänggi, and D. Tannor, *Chem. Phys.* **217**, 117 (1997).

¹⁶D. J. Tannor and S. A. Rice, *Adv. Chem. Phys.* **70**, 441 (1988).

¹⁷P. Brumer and M. Shapiro, *Annu. Rev. Phys. Chem.* **43**, 257 (1992).

¹⁸Y. Dakhnovskii, *Ann. Phys. (N.Y.)* **230**, 145 (1994).

¹⁹R. I. Cukier and M. Morillo, in *Molecular Electronics*, edited by J. Jortner and M. Ratner (Blackwell Science, Oxford, 1997), p. 119.

²⁰M. Grifoni and P. Hänggi, *Phys. Rep.* **304**, 229 (1998).

²¹M. Morillo, C. Denk, and R. I. Cukier, *Chem. Phys.* **212**, 157 (1996).

²²R. I. Cukier, C. Denk, and M. Morillo, *Chem. Phys.* **217**, 179 (1997).

²³D. A. McQuarrie, *Statistical Mechanics* (Harper & Row, New York, 1976).

²⁴R. Kubo and Y. Toyozawa, *Prog. Theor. Phys.* **13**, 60 (1955).

²⁵N. S. Hush, *Prog. Inorg. Chem.* **8**, 391 (1967).

²⁶N. Sutin, *Prog. Inorg. Chem.* **30**, 441 (1983).

²⁷R. Jankowiak, J. M. Hayes, and G. J. Small, *Chem. Rev.* **93**, 1471 (1993).

²⁸D. A. Wiersma, W. P. de Boeij, and M. S. Pshenichnikov, *Annu. Rev. Phys. Chem.* **49**, 99 (1998).

²⁹R. I. Cukier and M. Morillo, *Phys. Rev. B* **57**, 6972 (1998).

³⁰M. Morillo and R. I. Cukier, *J. Chem. Phys.* **110**, 7966 (1999).

³¹R. Kubo, in *Fluctuations, Relaxation and Resonance in Magnetic Systems* (Plenum, New York, 1962).

³²R. Kubo, *Adv. Chem. Phys.* **15**, 101 (1969).

³³J. Ulstrup, *Charge Transfer Processes in Condensed Media* (Springer-Verlag, Berlin, 1979).

³⁴V. G. Levich, in *Physical Chemistry—An Advanced Treatise*, edited by H. Henderson and W. Yost (Academic, New York, 1970), Vol. 9B, p. 985.

³⁵B. Fain, *Theory of Rate Processes in Condensed Media* (Springer-Verlag, Berlin, 1980).

³⁶A. O. Caldeira and A. J. Leggett, *Ann. Phys. (N.Y.)* **149**, 374 (1983).

³⁷L. Landau and E. M. Lifshitz, *Statistical Physics* (Pergamon, Oxford, 1980), Part I, Sec. 124.

³⁸H. Frölich, *Theory of Dielectrics* (Oxford University Press, London, 1958).

³⁹M. C. Wang and G. E. Uhlenbeck, in *Selected Papers on Noise and Stochastic Processes*, edited by N. Wax (Dover, New York, 1954).

⁴⁰M. Morillo and R. I. Cukier, *J. Chem. Phys.* **98**, 4548 (1993).

⁴¹The connection between Hamiltonian and stochastic methods can be obtained with some generality; see for example, E. Cortés, B. J. West, and K. Lindenberg, *J. Chem. Phys.* **82**, 2708 (1985).

⁴²N. G. van Kampen, *Stochastic Processes in Physics and Chemistry* (North-Holland, Amsterdam, 1992).

⁴³J. C. Tully, *J. Chem. Phys.* **93**, 1061 (1990), and references therein.

⁴⁴R. I. Cukier and M. Morillo (manuscript in preparation).

⁴⁵R. I. Cukier and M. Morillo, *Chem. Phys.* **183**, 375 (1994).

⁴⁶R. L. Honeycutt, *Phys. Rev. A* **45**, 604 (1992).

⁴⁷M. Morillo and R. I. Cukier, *J. Chem. Phys.* (submitted).